Optimising an Akpo Lobe Reservoir Static Model to Align with Dynamic Behaviour

Robyn Evans*[1], Jean-Michel Kluska[2], Vincenzo Spina[1], Chukwuka Chizea[1] and Mobolaji Fashanu[1]
[1]TotalEnergies EP Nigeria Limited
[2]TotalEnergies OneTech France

ABSTRACT

This paper focusses on the static modelling of one of the reservoirs within the Akpo Field, Block PML 2, offshore Nigeria. The reservoir is part of a deepwater turbidite lobe complex that dates from the Late Oligocene to Mid-Miocene, with good petrophysical properties (~20% Porosity and ~800mD permeability). The reservoir has been represented by several updated models since 2003, due to the various seismic campaigns and additional geological information derived by new wells drilled over the field. In recent years, the pore volume within the dynamic reservoir model has been increased in order to match production data. A recent rebuild of the static reservoir model was undertaken in 2023 to ensure the coherency between remaining reserves and comprehension of the field behaviour under dynamic conditions. This enabled an optimisation of the reservoir management and potential new infill opportunities to be considered. Presented here are some lobe-specific static modelling incoherencies observed within the previous model version compared to field data. Solutions to the identified incoherencies are discussed and the qualitative impact these solutions have on the reservoir model pore volume are described.

Keywords: Production Geology, Reservoir Geology, Reservoir Modelling, Static Model, Akpo Field, Pore Volume, Turbidite Lobe, Lobe Elements, Quartz Cementation, Diagenesis

THE AKPO FIELD GEOLOGICAL SETTING AND INTRODUCTION

The Akpo Field, within block PML 2, was discovered in 1999 and is located 135km from the Nigerian coastline at a water depth of 1400m (Figure 1). The field is jointly owned by the Nigerian National Petroleum Corporation (NNPC), South Atlantic Petroleum Limited (SAPETRO), PRIME 130, Chinese National Offshore Oil Corporation (CNOOC) and Total Upstream Nigeria Limited (TUPNI), the technical operator.

The Akpo Field comprises a 50km2 four-way dip anticline structure induced by shale diapirism. The Akpo field was initially appraised by four wells with an evaluation of reserves estimated at 620 Mbbls. The hydrocarbon fluid is principally condensate with some gas reserves.

Akpo comprises six main vertically stacked reservoirs in laterally offset positions, with a range of structural and stratigraphic trapping mechanisms (Figure 2).

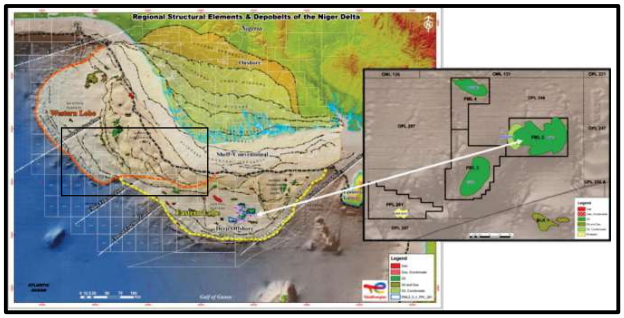

Figure 1: Regional Structural Elements & depobelts of the Niger Delta with the location of the Akpo Field within Block PML 2, Nigeria.

The reservoir level discussed in this paper is R5, one of the deepest within the Akpo Field. This reservoir is characterized by stacked lobe complexes with a gross thickness of 100m and is situated centrally over the Akpo anticline. The reservoir has a single oil-water contact (OWC) and is developed by four producers and supported by two water injectors. R5 is significant as it has one of the highest ultimate recovery factors at >60%, accounting for a third of Akpo's field production.

Since 2003, the R5 has been represented by several reservoir models which have been refined due to the The

The authors wish to thank NNPC Limited, NNPC Upstream Investment Management Services (NUIMS), TotalEnergies EP Nigeria Limited, TotalEnergies OneTech, France and NAPE for providing the platform to present the paper during the Annual Conference.

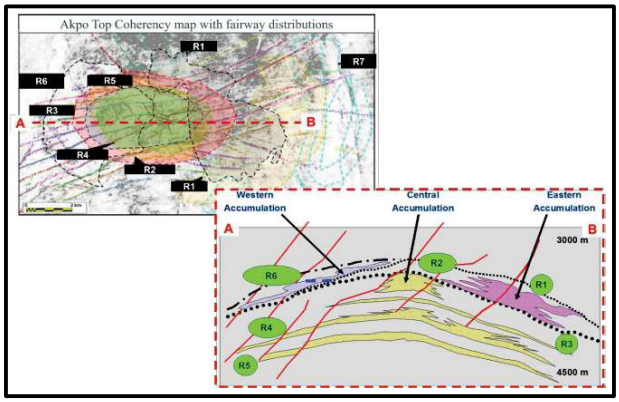

Figure 2: The main Akpo reservoir series (R1 to R6) stacked vertically over the anticline (Late Oligocene to Mid-Miocene in age).

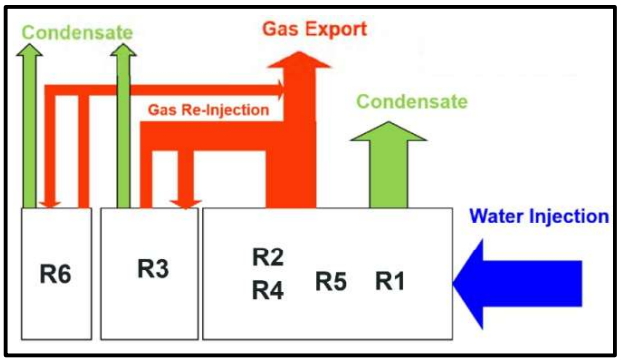

Figure 3: Akpo Field pressure maintenance: 20 water injectors and 2 gas injectors.

Today, 51 wells have been drilled over the Akpo structure, 44 FDP and 7 Infill. Akpo is a mature field requiring continued efforts in reservoir management to optimise production in its late development phase. The field pressure is maintained by water and gas re-injection (Figure 3).

The reservoir reservoir level discussed in this paper is R5, one of the deepest within the Akpo Field. This reservoir is characterized by stacked lobe complexes with a gross thickness of 100m and is situated centrally over the Akpo anticline. The reservoir has a single oil-water contact (OWC) and is developed by four producers and supported by two water injectors. R5 is significant as it has one of the highest ultimate recovery factors at >60%, accounting for a third of Akpo's field production.

Since 2003, the R5 has been represented by several reservoir models which have been refined due to the continued acquisition of well and seismic data over the field. In recent years, the pore volume within the dynamic model has been increased to match production data. To be able to optimize the R5 reservoir management and discover potential new infill opportunities, the static model was rebuilt in 2023 to ensure coherency between remaining reserves and comprehension of the field behaviour under dynamic conditions.

This paper discusses key lobe-related static modelling incoherencies observed within the previous model compared to field data, the proposed solutions to the problems, and the qualitative impact that these solutions have on the newly rebuilt reservoir model regarding pore volume and the representation of geological heterogeneities.

	Reservoir model incoherencies observed in previous version	Solution for static model rebuild	Impact on the new static model
1	Structural horizons not matching new seismic	• Refine structure	Slight decrease in model PV & So
2	Architectural element boundaries not matching new seismic	• Refine boundaries	Increase in model PV
3	Field scale geological heterogeneities: Globally connected but indirect injector → Producer pathways (not fully understood)	• 2G&R synthesis to identify dynamically important elements to represent in the model	Increase in vertical & horizontal heterogeneity
4	Grid resolution – Architectural Elements: • Evolve vertically at resolution smaller than defined modelled units	• Architectural Elements respect sequence stratigraphy irrespective of unit definition	Increase in vertical & horizontal heterogeneity Decrease in model PV
5	Grid resolution - Lobe Element (log scale): • 'Lobe Element' geobodies not optimally represented • Vertical cell resolution doesn't capture all individual laminate facies	• Minimum resolution reached to optimise Lobe Element representation • Cut off used on Petrophysics data to remove shale fraction from 'Reservoir' cells • Log scale facies proportions & petrophysical distributions used as targets in modelling	Increase in vertical & horizontal heterogeneity Increase in model PV Increase in model PV
6	Discretisation of petrophysical data: Bimodal distribution if Oil & Water modelled together due to diagenesis	• Porosity modelled separately; different mean distributions & burial compaction gradients per facies for Oil & Water	Increase in model PV

Figure 4: Inventory of static modelling incoherencies observed in the previous R5 reservoir model of the lobe reservoir, proposed solutions and the impact on the new static model.

A summary of static reservoir model incoherencies observed in the previous model version.

Figure 4 illustrates a summary of incoherencies observed in the previous version of the static model compared to field data. Items 3 to 6 highlighted in red will be discussed in detail as they present learning opportunities for model optimisation which are lobe-specific and case-specific to the R5 reservoir discussed in this paper.

Field scale geological heterogeneities: optimising the understanding of reservoir connectivity in the grid and its proposed impact on the model

The first static model optimisation opportunity to be discussed is described in Figure 4 (point 3) as 'Field scale geological heterogeneities'. This refers to the representation in the grid of faults and stratigraphy and their relationship. The interaction of these features plays an important role dynamically at the field scale, especially within this turbidite lobe reservoir due to the frequent alternating sand and shale units.

Even though dynamic data demonstrates that the R5 reservoir is connected at the field scale (i.e. production, pressure and 4D data), the injector-producer pathways are indirect, and it is this complex phenomenon which was not fully captured in the previous model. To improve the understanding of the reservoir connectivity, a synthesis was undertaken which enabled the characterization of some faults as 'dynamically important'. These faults were then modelled explicitly in the new model, with special attention made to validate their fault-stratigraphy relationships along the throw.

Figure 5 shows a schema of the R5 reservoir stratigraphy illustrating the superimposition of five vertical units. The Lower and Middle units are made up of several stacked lobe complexes, creating a well-connected homogeneous

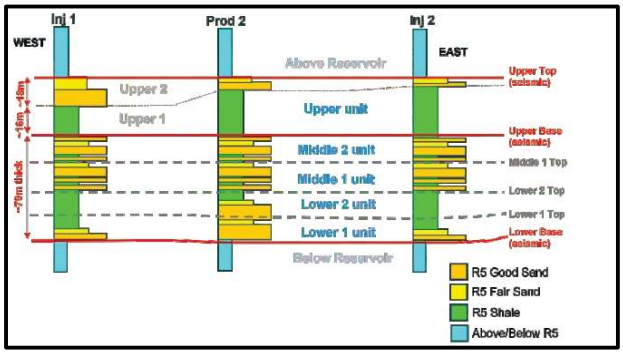

Figure 5: Akpo R5 reservoir stratigraphy: the five vertical units behave as two connected units.

sand interval (~70m thick); often referred to as the Mid/Low unit. The Upper unit comprises two intervals: a shaly interval named Upper 1 at the bottom (~15-20m thick), overlain by a sand-rich interval named Upper 2 (~20m thick). The Upper 2 interval has been recognized in the Western sector of the Akpo Field, with a lateral degradation towards the east. Despite the presence of this thick regional shale in between the Mid/Low and Upper 2 units, dynamic data has shown that vertical connectivity does occur via some key faults.

Figure 6 illustrates recent 4D seismic data within the

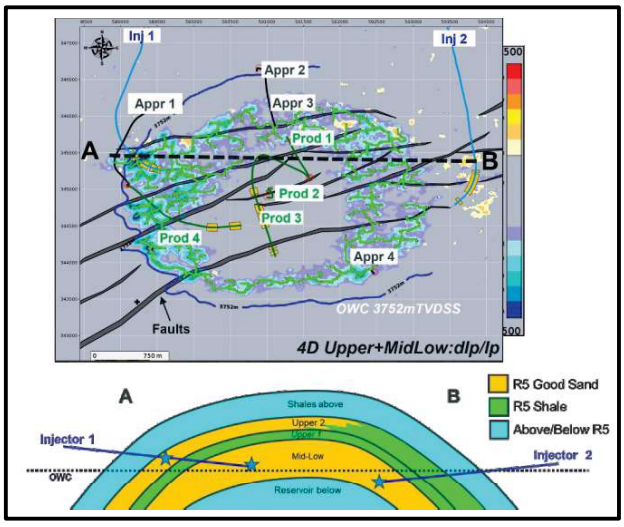

Figure 6: Connectivity tool performed on recent 4D seismic data demonstrates a globally connected R5 reservoir irrespective of the initial 'seed' location.

Mid/Low and Upper R5 reservoir units. Within the 4D signal are green lines which are the result of a connectivity tool that propagates connected pathways through the 4D seismic data. The starting points are known as the 'seed', which are placed at the injector locations. Overlain on the 4D are faults characterized as normal, north-westerly dipping and with variable throws. The schematic cross-section in Figure 6 displays the location of the three completion intervals along the two water injectors (blue stars) in relation to the Mid/Low and Upper reservoir levels.

The results of the connectivity tool show that irrespective of the initial seed placement within the different reservoir units, the green pathways always have the same pattern. This suggests that the R5 reservoir and its subunits are globally in vertical and lateral connection. This is further supported by the R5 global pressure data recorded through time, which is today at around 360 bars.

However, when taking a closer look, we have also observed in dynamic and 4D seismic data that some faults play a key role in assisting or hindering fluid connectivity, by creating tortuous pathways around the reservoir. This is evident in Figure 6 where the 4D data shows anomalies discontinuing along the faults to the West.

Since there are no erosive surfaces, for connectivity to occur between the Mid/Low and Upper 2 units across the Upper 1 regionally thick shale interval, the Upper 2 sand

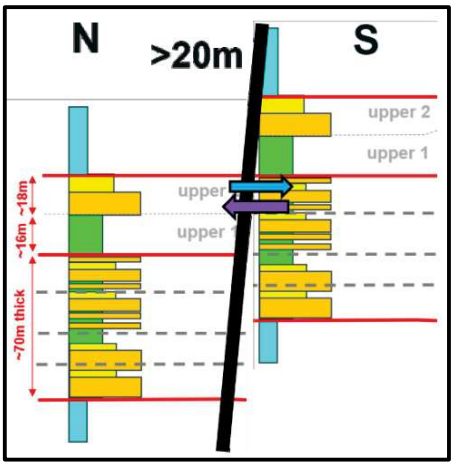

Figure 7: Faults with a throw of >20m enables 'vertical' Reservoir connectivity between the Mid/Low and Upper 2 units.

interval must be downthrown by faults with a minimum of 20m to the North against the Mid/Low unit. Figure 7 shows a schema of this interaction between the reservoir stratigraphy and a normal fault with a throw greater than 20m. Using this principal, all R5 faults with a minimum throw of 20m were identified through a seismic fault-throw analysis, and dynamically important faults were then identified. The intra- and inter-unit connectivity was then studied, resulting in an improved understanding and field mapping of the connectivity, vertically and laterally around the R5 reservoir.

Figure 8 shows a resulting summary of the fault throw-

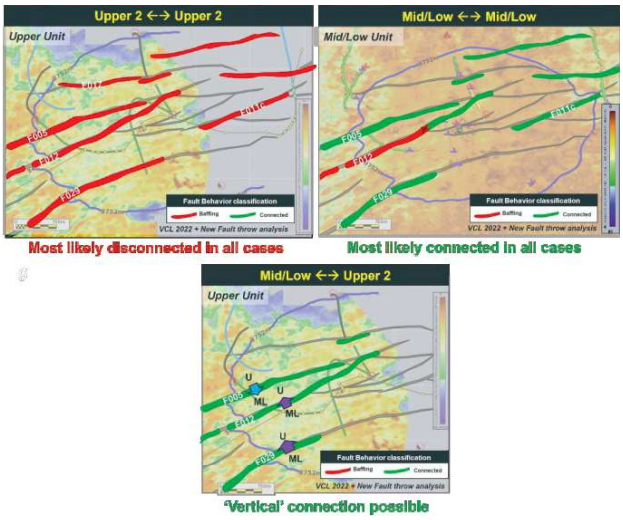

Figure 8: The fault-stratigraphy relationship plays a key role in understanding field scale connectivity of lobe reservoirs due to the alternating sand and shale strata.

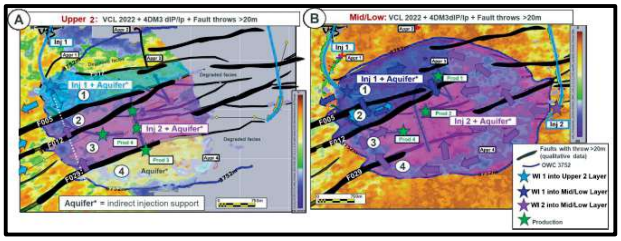

Figure 9: Three main western faults influence different regions of pressure support within the Upper 2 and Mid/Low reservoir units.

stratigraphy study, which describe the most likely connections within and between the Upper 2 and Mid/Low units.

The fault throw-stratigraphy study results were then consolidated with 4D and dynamic data to propose a hypothesis of different regions of pressure support (Figure 9).

Figure 9 'A' demonstrates that the Upper 2 interval is likely to have three regions of pressure support, influenced principally by three dynamically important faults (F005, F012 and F029). Whilst Figure 9 'B' demonstrates that the Mid/Low unit is likely to have two main regions of

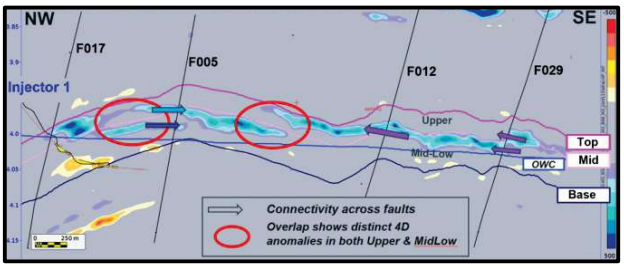

Figure 10: Section showing connectivity across 'dynamically important' faults supported by 4D data.

pressure support influenced by one dynamically important fault (F012).

This finding is further supported when analyzing cross sections of the interactions between the 4D seismic data versus faults and stratigraphy. Figure 10 displays a northwest-southeast cross section through the reservoir. The 4D signal can be seen to pass between the Mid/Low and Upper 2 units across the dynamically important faults F005, F012 and F029, as predicted in the fault throw-stratigraphy study.

Explicitly modelling the faults identified to have a dynamic impact more rigorously with regards to their location, extension and stratigraphic fault throw relationships in the new grid, has led to an improved predictability of the model dynamic behaviour at the field scale.

Grid Resolution: optimising the representation of lobe architectural elements in the grid and its proposed impact

This next section discusses optimising the representation of lobe architectural element turbidites (AET's) with regards to their vertical resolution within the static grid.

It was observed in the previous model that the lateral boundaries of the AET's of the R5 Lower 1 interval were inconsistent with the vertical facies' changes in the regional log data; the AET's were modelled with stationary

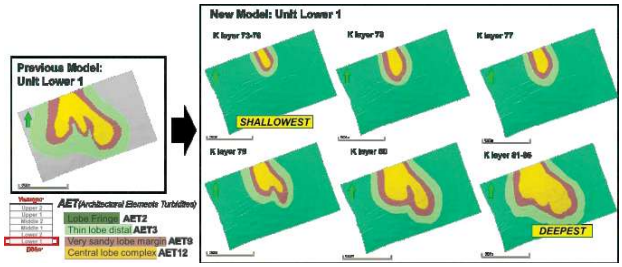

Figure 11: The R5 reservoir AET's: Lower 1 interval AET's modelled as non-stationary in new model versus stationary in the previous model.

boundaries for the entire Lower 1 interval, whereas log data was indicative of an intra-unit transgressive event.

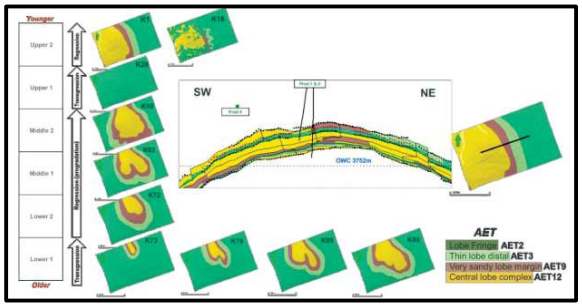

Figure 12: AET's in the new model respect the reservoir sequence stratigraphy observed at seismic and log scale.

When integrating log data with a resolution smaller than the defined vertical grid units, AET boundaries can be refined to better represent the sequence stratigraphy of the reservoir. Figure 11 shows the stationary AET boundaries of the previous model compared to the revised non-stationary boundaries in the new model for the Lower 1 interval. The updated AET boundaries are seen to reduce in size towards the shallowest 'K' layer.
Figure 12 displays the AET's for all reservoir units, with optimised intra- and inter-unit sequence stratigraphy supported by log data.
The impact of revising the AET vertical resolution on the new model has led to an improvement in the representativeness of the vertical and horizontal geological heterogeneities within the Lower 1 interval. Additionally, the pore volume sees a slight decrease due to the reduction in sand proportion towards the top of the interval.

Grid Resolution: optimising the representation of lobe elements in the grid and its proposed impact
This next chapter discusses optimizing the representation of lobe elements both horizontally and vertically within the grid.

1. Horizontal resolution of lobe elements
Turbidite lobe complexes are made up of sub-environments within a fivefold hierarchy system

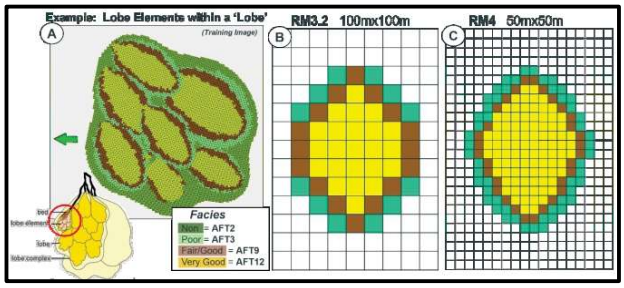

Figure 13: Lobe elements represented at the horizontal grid scale (schema of lobe sub-environments by Spychala *et al.,* 2021).

(Spychala et al., 2021). The smallest sub-environment to be represented at the grid scale within the static model is the lobe element. Several lobe elements that are divided by thin siltstone intervals form a lobe, and several stacked lobes form a lobe complex. The small schema in

Figure 13 describes this hierarchal system (Spychala et al., 2021). Displayed also is how the lobe elements are represented within the grid when they are stacked together to create a lobe (A) and modelled individually at different horizontal cell resolutions (B and C).

A lobe element is typically oval with model dimensions of approximately 700mx900m in width and length respectively for the R5 reservoir. The facies of a lobe element are organized with a very good facies at its center, followed by a fair/good facies at its border and a poor facies on the periphery.

The individual lobe elements modelled in the grid (Figure 13B and 13C) demonstrate the difference between modelled bodies in the previous version with a horizontal cell resolution of 100x100m, compared to a newly proposed finer cell resolution of 50x50m. The facies organization is better respected at the finer cell resolution, supporting the decision to implement a horizontal cell size of 50x50m in the model rebuild.

Optimising the geological representation of lobe elements in the grid will likely improve the predictability of the internal dynamic reservoir behavior.

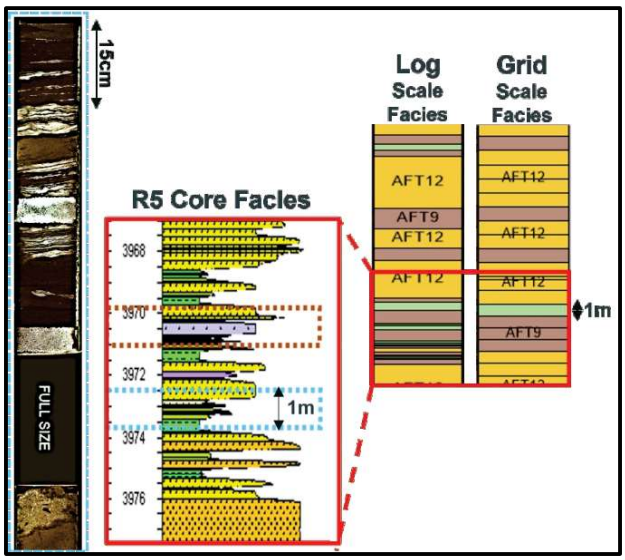

Figure 14: Alternating sand and shale facies within a laminated interval of the R5 reservoir at the core, log and grid scale.

2. Vertical resolution of lobe elements and upscaling considerations
Removing the shaly fraction at the log scale to better estimate the mean target petrophysical properties of the reservoir facies:

The next component of this chapter discusses best practices to avoid bias at different stages of the upscaling process, due to the frequent alternation of fine shales and sands within turbidite lobe facies.
Figure 14 illustrates a core lithology sample with alternating sand and shale laminae below the resolution of 15cm. 15cm is the typical frequency of petrophysical log measurements, which means at the log scale, the representativity of the facies is dependent on where the sampling occurs along the lithology. If a sampling bias occurs where a higher frequency of shale laminae are

sampled instead of sand, the petrophysical values in reservoir intervals at the log scale may be diluted by shales.

To better characterize the petrophysical properties of the R5 reservoir facies, A cut-off is applied to a sand fraction log calculated using the Thomas-Stieber model; an optimal NTG method in thin bed turbidite contexts (for a detailed description of the Thomas-Stieber model refer to Ghaleh *et al.,* 2017). The Thomas-Stieber model provides a sand fraction log with continuous values from 0 to 1, compared to conventional binary NTG logs. When applying a cut-off of 0.3, the non-reservoir fraction is removed and a distribution of the mean log-scale petrophysical properties of the sand fraction are obtained

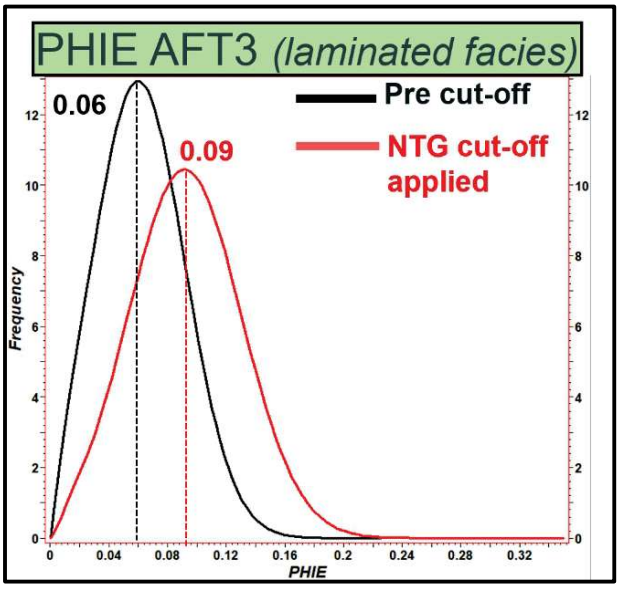

Figure 15: Applying a cut-off on the Thomas-Stieber NTG log to remove the shaly fraction, enables a better estimate of the mean petrophysical properties of the R5 reservoir facies for modelling at the grid scale.

per reservoir facies. These distributions can then be used as targets for petrophysical modelling for the reservoir facies in the grid.

This has the biggest impact in laminated facies, such as AFT3, where the petrophysical mean is more heavily diluted by the presence of fine shales. Figure 15 demonstrates the impact of applying a cut-off on the effective porosity (phie): prior to applying the cut-off, the mean value of phie is 0.06 porosity units (p.u.) compared to a mean value of 0.09 p.u. post cut-off.
Using petrophysical means from cut-offs as targets in petrophysical modelling enables the characteristics of the reservoir facies to be better represented at the grid scale, the pore volume is better estimated and the connectivity within the model is better captured.

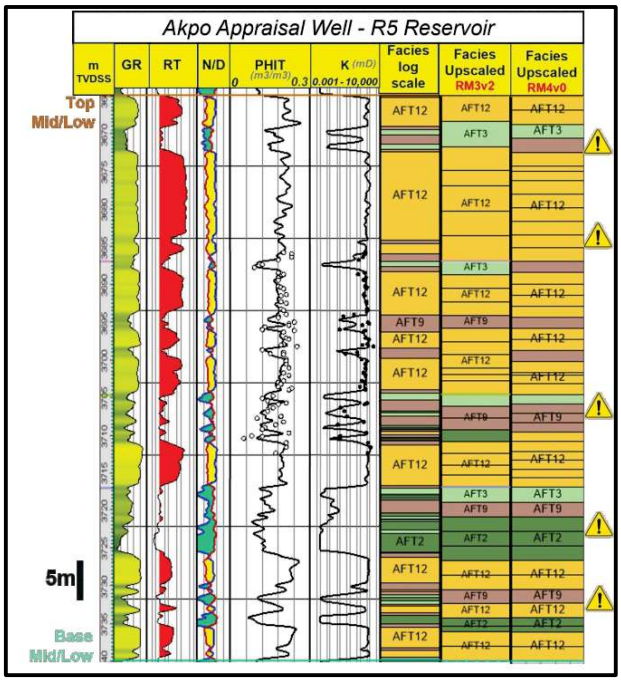

Figure 16: The vertical resolution of the new grid RM4v0, better captures the log scale facies of the R5 reservoir, but is unable to capture all the finer laminated facies.

Reduce the vertical cell resolution to better capture the vertical geological heterogeneities of the facies logs:
The vertical cell resolution is an important consideration when upscaling electro-facies logs into the grid, espeially in turbidite lobe environments where thinner alternations of sand and shale are frequent. In order to best capture these thinner facies, the vertical cell resolution was refined in the new grid to an average thickness of 1.26m compared to 1.60m in the previous model.

Figure 16 shows the result of facies upscaling between the new model (RM4v0) and previous model (RM3v2). A higher proportion of laminate facies is captured within the new grid due to the reduction of the vertical cell resolution compared to the previous model. It is therefore recommended to take the vertical grid as fine as possible, whilst considering the risk of pinched cells and avoiding to exceed the maximum recommended number of grid cells for reservoir simulation.

Despite the finer new grid, not all facies are captured. Figure 16 demonstrates missing facies in the upscale domain compared to the log scale (marked by exclamation points). These facies are below the resolution of a resonable vertical grid cell size. The impact of this grid limitation on upscaling the log scale is discussed more below

Use logscale facies proportions to drive facies modelling:
Figure 17 illustrates the difference in facies proportions

between the log scale and upscale domains within the new grid vertical layering. Some comparisons show an

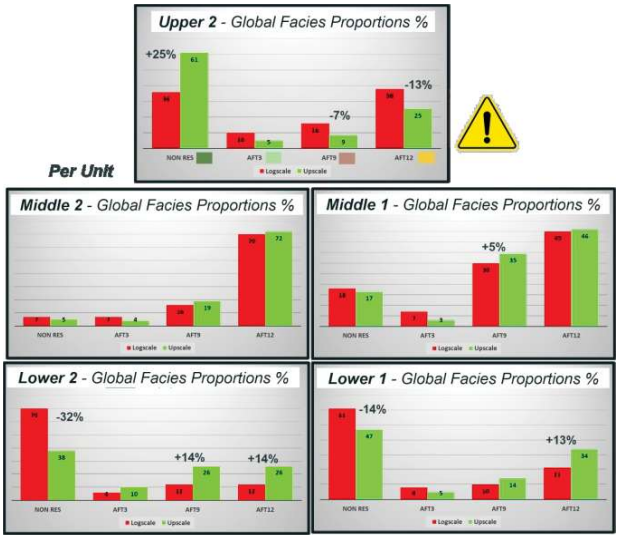

Figure 17: The facies proportions resulting from the upscaling in the new grid show unacceptable matches with the log scale proportions.

unacceptable match with either an over- or under-estimation of the log scale facies proportions in the grid (i.e. 13% less AFT12 in the Upper unit).

The reason for such a discrepancy in proportions is due to the frequence of laminated facies in lobe turbidite environments which are captured at the log scale, but fall below the resolution of the vertical grid cells. It is therefore recommended to respect log scale facies proportions as targets for facies modelling to avoid any misrepesentation due to the upscaling process.
Ensuring that the log scale proportions drove the facies modelling in the new R5 model, led to a global increase in pore volume, mainly attributed to the Upper 2 reservoir interval.

Discretizing petrophysical data due to diagenesis and its proposed impact on the reservoir model

The final static model optimisation opportunity to be discussed is the discretization of petrophysical data due to diagenesis. Although this regards the R5 reservoir discussed in this article, it is unlikely to be case specific to turbidite lobe reservoirs only. Nonetheless, the phenomenon is discussed here due to the noteworthy impact it has on the model pore volume.

Figure 18 shows a bivariate plot of log PHIT versus burial depth for the fair/good and good reservoir facies in the R5. Two trends can be observed (red lines), separated by a decrease and change in gradient at the R5 OWC. The univariate plot 'A' is log data for the good facies from the oil leg and 'B' is log data from the good facies from the water leg. A difference can be observed in the mean

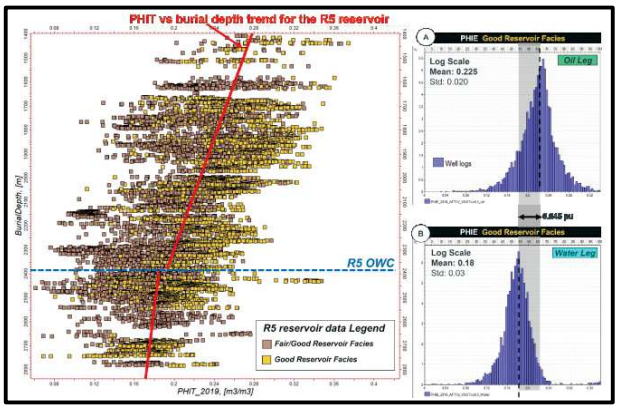

Figure 18: R5 reservoir petrophysical log data is discretized by facies and by the oil and water leg.

porosity values between the two univariate plots: the mean phie value in the water leg is 0.18 p.u. compared to 0.225 p.u. in the oil leg. This 0.045 p.u. difference in porosity can in part be attributed to the porosity evolution controlled by mechanical compaction. But the change in gradient of the PHIT versus burial depth below the OWC (red trend in Figure 18) suggests that diagenesis also plays a role in the degradation of porosity in the water leg. Since oil saturation can inhibit or slow down the occurrence of quartz cementation, diagenesis is more evident in the water saturated porosity.
Figure 19 displays a bivariate plot of porosity data from all Akpo reservoirs versus burial depth. The blue dashed curve represents the porosity evolution of moderately sorted sandstones controlled by mechanical compaction (Paxton *et al.,* 2002). Once the reservoir reaches a burial depth with a temperature of 70°C, quartz cementation may start to occur (if uninhibited by the presence of oil); with increased efficiency at higher temperatures (80°C to 90°C) (Oye *et al.,* 2020).

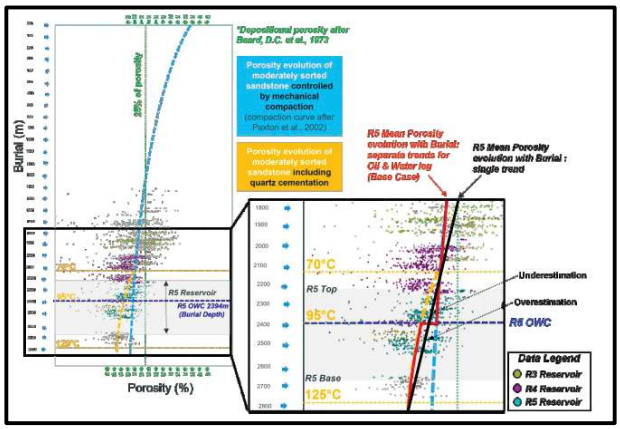

Figure 19: Log data of porosity evolution with burial depth shows a change at the OWC due to quartz cementation in the reservoir.

At the OWC of the R5 reservoir (2394m burial), the

temperature is approximately 95°C i.e. ideal conditions for quartz cementation. The porosity data versus burial of all Akpo reservoirs can be seen to follow the porosity evolution of moderately sorted sandstone controlled by mechanical compaction (blue dashed curve) until the OWC of the R5 reservoir. Below the OWC, the R5 porosity data then follows the porosity evolution of moderately sorted sandstone including an impact from quartz cementation (orange dashed curve).

By better understanding the evolution of porosity versus burial in the R5 reservoir, a two-part mean trend was constructed (red line in Figure 19) with a change in gradient to respect the shift from 'mechanical compaction' to 'mechanical compaction with quartz cementation' at the R5 OWC. This new trend was then used to model the porosity evolution with burial in the new R5 model, which corrected the overestimation of the porosity in the water leg and underestimation of the porosity in the oil leg (seen in the single mean black trend). This impacted the pore volume by increasing it in the R5 reservoir facies above the OWC.

Figure 20 illustrates thin section micrographs from the R5

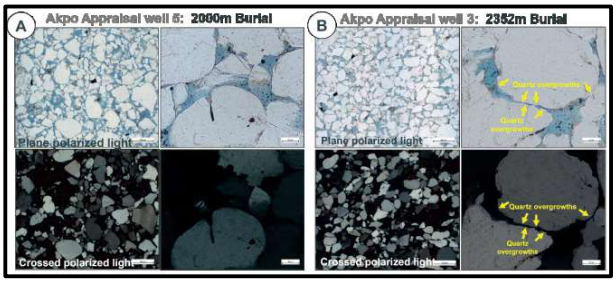

Figure 20: Thin sections illustrating quartz overgrowths in reservoir R5at two different burial depths.

reservoir in two appraisal wells. The thin section labelled 'A' is from a burial depth of 2000m (below the 70°C threshold of quartz cementation) and illustrates limited to no evidence of quartz cementation. The thin section labelled 'B' is from a burial depth of 2352m (approaching the 95°C reservoir temperature) and shows evidence of several thin quartz overgrowths. This demonstrates that even at a high oil saturation, the quartz cementation is starting to show just above the OWC of the R5 reservoir, below which the cement proportion most likely increases sharply within the water leg (as demonstrated in Figure 19).

CONCLUSION

Production data from the R5 reservoir showed an increase in volumes over the last few years compared to the static appraisal, leading to an overall increase in pore volume multipliers applied in the dynamic model. A rebuild of the static model was required to ensure coherency between remaining reserves and the comprehension of the field behaviour under dynamic conditions.

The static model rebuild approach scrutinized the input of small- and large-scale data (log to seismic) and identified key incoherencies in the static modelling of turbidite lobes from the previous model version compared to field data. Addressing these challenges helped optimise the representation of the turbidite lobe reservoir and important geological heterogeneities in the grid, which consequently led to an increase in the dynamic predictability of the model and overall static pore volume.
The main static model components that were optimised and outlined in this paper are summarized:

- The 2G&R synthesis demonstrated the dynamic importance of explicitly modelling three main faults due to their significant impact on the injector to producer pathways though the reservoir.
- The lateral and vertical grid resolution plays an important role in how lobe reservoirs and their varying scales of heterogeneities are optimally represented within the model.
- Applying a cut-off on petrophysical data to remove the shaly fraction, especially in laminate facies, enables a better characterization of the turbitide lobe reservoir facies to be represented in the reservoir cells.
- When discretizing the facies groups, potential diagenetic changes related to burial depth, temperature and fluid saturation should be considered as this can have a significant impact on reservoir petrophysical properties.

REFERENCES CITED

Beard D.C., and Weyl P.K. (1973) - Influence of texture on porosity and permeability on unconsolidated sand. Am. Assoc. Pet. Geol. Bull., 57, 349–369.

Ghaleh, S.P., Taghizadeh, M., Far, E.R, Kordavani, A. and Mirzaei, M. (2017) - Evaluation of laminated shaly sand sequences in Ahwaz oil field using (via) Thomas Stieber method and conventional petrophysical logs. Journal of Petroleum Science and Engineering, 152, 564-574.

Oye, O. J., Aplin, A.C., Jones, S.J., Gluyas, J.G., Bowen, L., Harwood, J., Orland, I.J. and Valley, J.W. (2020) - Vertical effective stress and temperature as controls of quartz cementation in sandstones: Evidence from North Sea Fulmar and Gulf of Mexico Wilcox sandstones. Marine and Petroleum Geology, 115, 104289.

Paxton S. T., Szabo J. O., Ajdukiewicz J. M. and Klimentidis R. E. (2002) - Construction of an Intergranular Volume Compaction Curve for Evaluating and Predicting Compaction and Porosity Loss in Rigid-Grain Sandstone Reservoirs. AAPG Bulletin, 86, 2047–2067.

Spychala, Y.T., Ramaaker, T. A. B., Eggenhuisen, J. and Grundvag, S.A., (2021) - Proximal to distal grain-size distribution of basin-floor lobes: A study from the Battfjellet Formation, Central Tertiary Basin, Svalbard. The Depositional Record, 8, 436–456.